Insights on the use of metal complexes of thiourea derivatives as highly efficient adsorbents for ciprofloxacin from contaminated water

Journal:	*Transactions of the Royal Society of South Africa*
Manuscript ID	TTRS-2018-0058.R1
Manuscript Type:	Original papers
Keywords:	Thiourea, ciprofloxacin, metal complexes, adsorption, remediation

Insights on the use of metal complexes of thiourea derivatives as highly efficient adsorbents for ciprofloxacin from contaminated water

Kovo G. Akpomie[1], Omotola M. Fayomi[2], Chidinma C. Ezeofor[1,3], Rufus Sha'Ato[2] & Werner E. Van Zyl[4]

[1]Department of Pure & Industrial Chemistry, University of Nigeria, Nsukka, Nigeria

[2]Department of Chemistry, University of Agriculture Makurdi, Benue State Nigeria

[3]Department of Chemistry, University of Pretoria, Pretoria, South Africa

[4]School of Chemistry and Physics, University of KwaZulu-Natal, Westville Campus, Durban 4000, South Africa

Correspondence to: omotolafayomiatgmail.com

Abstract

Despite the wide use of synthesised metal complexes of thiourea and their derivatives in medicine and corrosion inhibition, a paucity of research exists on their application as adsorbents for pollutants. This study was aimed at investigating the adsorption potential of the copper (II) and zinc (II) complexes of 4-nitro-substituted thiourea derivatives of aminophenol for ciprofloxacin (CPF). The metal complexes were synthesised and characterised. Fourier transform infrared spectroscopy, scanning electron microscopy and a BET surface area analyzer were utilised to determine the surface structure and properties of the synthesised adsorbents. Isotherms were conducted by the application of Langmuir, Freundlich and Scatchard models and revealed a heterogeneous multilayer adsorption process. Kinetic evaluation showed best fit with the pseudo second order model ($R2 > 0.991$) compared to the pseudo first order and Bangham equations. Thermodynamics showed an endothermic spontaneous abstraction process. The metal complexes showed over 80% desorption of CPF using 0.2 M NaOH and were stable over three cycles of regeneration and reuse. This research revealed the potential of the metal complexes of thiourea as adsorbents for CPF supported by the high adsorption capacity compared to other reported adsorbents

Keywords: thiourea, ciprofloxacin, metal complexes, adsorption, remediation

INTRODUCTION

The compounds produced in pharmaceutical industries constitute a harmful group of organic contaminants, since they are used extensively and regularly pollute the aquatic environment (Ashfaq et al., 2016). In animals and humans, several infectious diseases are widely treated by pharmaceutical products such as antibiotics (Darweesh and Ahmed, 2017). Several antibiotics are produced in large quantities and used as veterinary therapeutics in farms for animal growth enhancement (Wang et al., 2017). Most of the antibiotics are released eventually into the aquatic environment because only little amounts are metabolized by animal and human systems. A large amount of a given antibiotic may remain un-degraded in humans and animals and eventually be excreted as active substances (Pouretedal and Sadegh, 2014). Ciprofloxacin (CPF), a fluoroquinolone antibiotic has wide use in the treatment of a lot of bacterial infections such as diarrhea, skin irritations, joint and bone problems, typhoid fever, respiratory and urinary track disorders among others. This broad spectrum antibiotic has been detected frequently in effluents from hospitals, pharmaceutical industries and some rivers due to its extensive use (Wu et al., 2010; Carabinero et al., 2011). Despite the low concentration of CPF in the environment, it is known to cause antibiotic resistance in bacteria and chronic allergic reactions (Huang et al., 2014). Therefore, the removal of CPF from wastewater is necessary. Several techniques have been utilized for remediation of CPF and other contaminants from wastewater such as photo-fenton oxidation, ozonization, sonification, microbial remediation, chemical reduction and adsorption (Chen et al., 2011; Sturini et al., 2012; Li et al., 2014; Wu et al., 2015). The adsorption technique is the most commonly used and preferred due to its low cost, simplicity and effectiveness (Mao et al., 2016; Darweesh and Ahmed, 2017). Therefore, several adsorbents such as clay, zeolite, activated carbon, carbon nanotubes, silica, magnetic carbon, coal fly ash,

birnessite, graphene oxide, nanomaterials, calcium alginate, graphene oxide based nanomaterials, biomass materials and metal organic framework (MOF) have been utilized for the removal of various contaminants and CPF from solution (El-shafey et al., 2012; Wu et al., 2015; Sturini et al., 2016; Liang et al., 2016; Yu et al., 2016a; Darweesh and Ahmed, 2017; Khan et al., 2017; Gadipelly et al., 2018; Wu et al., 2019). However, some of these adsorbents recorded low adsorption capacity for CPF therefore the search for more adsorbents with high adsorption capacity continues (Gadipelly et al., 2018). Thiourea derivatives ligands are versatile compounds due to their vast properties as anti-tumor, anticancer, antiviral, antifungal, antibacterial and corrosion inhibition agents (Selvakumaran et al., 2013; de Oliverra et al., 2015). Furthermore, their metal complexes have shown enhanced activity in the various fields of application (Parmar et al., 2010). The structure of these metal complexes may be similar to MOF which are organo-inorganic hybrids with high porosity and large surface area formed from a metal salt with an organic linker or ligand (Hasan and Jhung, 2015). MOFs have been utilized effectively as adsorbents with superior adsorption capacity for contaminants when compared to most conventional adsorbents (Li et al., 2018; Gadipelly et al., 2018). It is therefore possible that the metal complexes of thiourea derivatives could have high adsorption capacity for CPF and other contaminants. However, despite the extensive use of the metal complexes of thiourea derivatives in medicine and corrosion, a thorough literature search revealed paucity of information on its application as adsorbents for contaminants. Although thiourea modified adsorbents and the formaldehyde hybrids resins have successfully been used and showed high adsorption for dyes and metal ions (Gezer et al., 2011; Muslu and Gulfen, 2011; Elwakeel et al., 2017; Elwakeel and Al-Bogami, 2018). This study was therefore conducted to evaluate the applicability of the some synthesized metal complexes of thiourea derivatives for the adsorption of CPF from aqueous

solution. The metal complexes were synthesized and characterized. Equilibrium, kinetic, thermodynamics and desorption studies were analyzed to evaluate the mechanism of CPF adsorption on the metal complexes.

MATERIALS AND METHODS

Reagents and instrumentation

Chemicals used for this work were obtained from different chemical suppliers. The 4-*nitro* benzoyl chloride were purchased from Sigma-Aldrich and supplied by Zayo-Sigma Chemical Limited Nigeria. Ammonium thiocyanate, 2-aminophenol, Cu (II) chloride dihydrate, and Zn(II) chloride were obtained from the chemical store of University of KwaZulu-Natal South Africa. Also, deuterated dimethyl sulphoxide (DMSO-d_6) was purchased from Merck Chemical Limited South Africa. All these reagents were used without further purification. Acetone was stored with molecular sieve 3A. Melting point was recorded on a Stuart Scientific apparatus SMP3 and is uncorrected. Infrared spectra were recorded using an ATR Perkin Elmer Spectrum 100 spectrometer between 4000 – 400 cm^{-1}. ^{1}H and ^{13}C NMR were recorded in DMSO-d_6 using TMS as an internal standard on a BRUKER 400 MHz spectrometer (AVANCE^{III} 400). NMR data are expressed in ppm (part per million) downfield shift. Scanning Electron microscopy of the synthesized metal complexes was determined by (SEM, Hitachi S4800 model), while the pore properties and surface area by the micromeritics ASAP surface area 2010 model analyzer.

Synthesis of *N*-(2-hydroxylphenyl)-*N'*-(4-nitro benzoyl) thiourea (HNT) (4)

The synthesis of *N*-(2-hydroxylphenyl)-*N'*-(4-nitro benzoyl) thiourea (HNT) (**4**) is shown in Scheme 1. This procedure was adapted from (Fayomi *et al.,* 2018a). A 1.52 g of Ammonium thiocyanate was prepared by dissolving in 10 mL of acetone. A 3.71 g of 4-*nitro* benzoyl

chloride (**1**) was dissolved in 30 mL of acetone separately. The two solutions were mixed gradually together. The mixture was heated under reflux for 2 hours, then cooled. The mixture was filtered. The 2-aminophenol **(3)** was added to the filtrate then refluxed for 2 hours. After which ice water was added to precipitate the product. The product was dissolved in dichloromethane and precipitated with ethanol solvent. The product mixture was filtered, washed with water and dried in the desiccators and labeled as HNT. Appearance: Brown Solid. Yield: 6.00 g (95 %); Melting point (172-173^{o}C). ^{1}H NMR, 400 *MHz* (DMSO-d_6), *ppm*: δ 8.34 (d, 1H, H-4), 8.57(m, 1H, H-5), 8.25 (d, 1H, H-7), 8.32 (d, 1H, H-8), 7.08 (d, 1H, H-11), 6.95 (m, 1H, H-12), 8.16 (m, 1H, H-13), 6.85 (d, 1H, H-14), 10.27 (d, 1H, 10-OH). ^{13}C NMR (DMSO-d_6), *ppm*: δ 177.05 (C-1), 168.81 (C-2), 138.06 (C-3), 126.53 (C-4), 123.00 (C-5), 148.84 (C-6), 118.31 (C-7), 130.25 (C-8), 135.70 (C-9), 149.75 (C-10), 115.08 (C-11), 123.39 (C-12), 123.24 (C-13), 125.82 (C-14).IR, ν (cm^{-1}): 3220 (N-H), 1724 (C=O), 1342 (C=S), 1654 (C=C), 1518 (N-O).

Synthesis of Cu (II) and Zn (II) complexes of HNT

The synthetic pathway (Scheme 2) for the Cu (II) complexes of HNT (**6**) involved the reaction of HNT (1.24 *m*mol) (in 15 mL ethanol) with ethanolic solution of copper (II) chloride dihydrate (0.62 *m*mol). The1.24 *m*mol of KOH was added to the mixture and continuously stirred at room temperature for 3 hr. The precipitate formed was filtered, washed with ethanol and dried under vacuum to constant weight. CuHNT Appearance: Green solid. Yield: 0.140 (17.50%). Melting point (165^{d} ^{o}C). IR, ν (cm^{-1}): 3107 (O-H), 1345 (C=S), 1608 (C=C), 1525 (N-O), 537 (M-S). For ZnHNT, Similar procedure was repeated to obtain zinc (II) complexes. Appearance: Grey solid. Yield: 0.054 (34.00%). Melting point (237-239 ^{o}C). IR, ν (cm^{-1}): 3359 (O-H), 1345 (C=S), 1634

(C=C), 1531 (N-O), 510 (M-S). These metal complexes were used as adsorbents for CPF abstraction.

Adsorption and desorption experiments

The adsorption of CPF on the adsorbents was carried out using batch techniques to study the effect of pH (2.0 – 10.0), ionic strength (0.1 – 0.3 M), initial ciprofloxacin concentration (100 – 500 mg/L), contact time (10 – 240 min) and temperature (300 – 323 K). The adsorption was performed by contacting 0.1 g of the adsorbent with 100 mL of 100 mg/L CPF solution at pH 6.0, room temperature 300 K and contact time 240 min. This was agitated at 150 rpm, the pH of the solution was adjusted using standard solutions of 0.1 M NaOH and 0.1 M HCl by checking with a pH meter. The effect of ionic strength was performed using NaCl solution while temperature influence was conducted in a water bath temperature regulator. At the end of the given agitation time, the solutions were filtered using membrane filters (0.45 μm) and CPF concentration in the filtrate was determined by the UV-visible spectrophotometer at a wavelength of 273 nm. Each experiment was conducted in triplicate and average values were calculated to ensure quality assurance. The percentage adsorption of CPF and adsorption capacity q_e (mg/g) of the adsorbent were calculated by the mass balance equation described (Dawodu and Akpomie, 2014).

The desorption of CPF was conducted by using 1.0 g of the adsorbent for adsorption of 100 mL of 1000 mg/L ciprofloxacin concentration at pH 6.0, agitation time 240 min and room temperature of 300K. After, the CPF loaded adsorbent was dried and obtained. The loaded sorbents were contacted with 150 mL of distilled water or 0.2 M NaOH solution and agitated for 2 hr after which it was filtered using 0.45 μm membrane filters. The concentration of

ciprofloxacin in the filtrate was then determined by the UV-Visible spectrophotometer and the percentage desorption calculated from the relationship

$$\% \, Desorption = 100[C_D V_D]/qem \qquad (1)$$

Where C_D (mg/L) represents the concentration of CPF in the desorbing solution, V_D (L) is the volume of desorbing solution used, q_e (mg/g) is the adsorption capacity of the CPF loaded adsorbent and m (g) is the mass of adsorbents utilized in desorption (Chukwuemeka-Okorie et al., 2018). The adsorbents after desorption were oven dried at 60 ^{0}C then reused for adsorption. Three cycles of adsorption-desorption experiments were conducted to determined the reusability of the metal complexes using 0.2 M NaOH as eluent.

All experiments performed were done in triplicate and the average values were calculated for quality assurance.

Equilibrium, kinetic and thermodynamic modeling

Equilibrium isotherm modeling of CPF adsorption unto CuHNT and ZnHNT was performed using the Langmuir (LM), Freundlich (FD) and Scatchard (SC) models while the kinetic modeling was carried out by the Pseudo-first order (PFO), Pseudo-second order (PSO) and Bangham (BH) equations. The respective model equations are given as:

$$C_e/q_e = 1/q_L K_L + C_e/q_L \qquad (2)$$

$$\log q_e = \log K_F + [1/n]\log C_e \qquad (3)$$

$$q_e/C_e = q_S b - q_e b \qquad (4)$$

$$\log (q_e - q_t) = \log q_e - (Kit/2.303) \qquad (5)$$

$$t/q_t = 1/K_2 q_e^2 + t/q_e \qquad (6)$$

$$\text{loglog}\,[C_i/(C_i - q_t m)] = \log (K_O m/2.303V) + a_B \log(t) \qquad (7)$$

Where q_L (g/g) is the LM monolayer uptake, K_L (L/g) is the adsorption constant, n the FD adsorption capacity, K_F (L/g) intensity, q_S (g/g) and b (L/mg) are the SC adsorption constants, qt (g/g) is the uptake capacity at time t (min), Ki (min^{-1}) is the PFO rate constant, K_2 (g/g/min) the PSO rate constant, V (ml), volume of solution, K_O (g) and a_B (< 1) are BH constants (Akpomie et al., 2018; Eze et al., 2019). Thermodynamic parameters such as free energy (ΔG˚), Enthalpy (ΔH˚) and Entropy (ΔS˚) were evaluated as described (Chukwuemeka-Okorie et al., 2018).

RESULTS AND DISCUSSION

Characterization of HNT, CuHNT and ZnHNT

The FTIR spectrum of HNT (**4**) had bands at 1724 and 1342 cm^{-1} assigned to carbonyl (>C=O) and thiocarbonyl (>C=S) groups respectively (Figure 1). These functional groups agree with the values in literature (Fayomi *et al.,* 2018). The FTIR spectra of CuHNT (**5**) and ZnHNT (**6**) are shown in Figure 2. The disappearance of the band assigned to carbonyl group has to do with the metal-ligand bonding in each of the complexes. A prominent band assigned ν(C=C) had a shift to lower wavelength (Omoregie et al. 2013). The existence of several functional groups on the metal complexes for interaction with CPF molecule suggests the potential of these adsorbents for efficient abstraction. BET analysis revealed surface areas of 1138 and 1003 m^2/g and total pore volume of 0.64 amd 0.61 cm^3/g for CuHNT and ZnHNT respectively. The surface area and pore volume although lower were close to that of zinc-benzenedicarboxylate a MOF with BET surface area of 1643 m^2/g and pore volume 0.69 cm^3/g (Gadipelly et al, 2018). The values obtained for both metal complexes were higher than that of activated carbon a reference

adsorbent with 642 m^2/g and 0.58 cm^3/g (Gadipelly et al., 2018). The high pore properties of both adsorbents suggest a high sorption potential for ciprofloxacin. The SEM images of the two metal complexes revealed a highly porous surface structure as shown in Figure 3. This was similar to that of the MOF utilized in the adsorption of ciprofloxacin from aqueous solution (Gadipelly et al., 2018). Again the high porous structures of both sorbents suggest high adsorption capacity for the contaminants (Chukwuemeka-Okorie et al., 2018).

Effect of pH and ionic strength on ciprofloxacin removal by the metal complexes

Solution pH plays an important role in the sequestration of pharmaceutical compounds from solution. The influence of solution pH on the removal of CPF by CuHNT and ZnHNT showed the pH affected the sorption process significantly as illustrated in Figure 4. An increase in percentage removal of CPF on both sorbent with pH was achieved up to pH 6.0 after which a significant decrease occurred from pH 8.0 to 10. Similar trend have been reported by other workers (Wang et al., 2011, Wang et al., 2017, El-shafey et al., 2012). pH 6.0 was chosen and utilized in all the adsorption experiment when the effect of other operating factors were studied. The dissociation constants for CPF at pKa_I and pKa_2 are 6.1 and 8.7 respectively. CPF molecules therefore exist as cations at pH values less than 6.1 due to protonation of the amine group (El-shafey et al., 2012). On the other hand, the carboxylic group losses a proton at pH > 8.7 causing the CPF molecule to be anionic in solution (Wang et al., 2010). The zwitterionic species of CPF occurs in the pH range of 6.1 – 8.7 (Wang et al., 2010). The low adsorption of CPF is attributed to the competition between the cationic CPF molecules and H^+ ions in solution and also less electrostatic attraction between positively charged adsorbent surfaces and cationic CPF. Adsorption in the pH range of 5.0 to 8.0 was due to electrostatic attraction between zwitterionic

CPF and CuHNT and ZnHNT. At higher pH, electrostatic repulsions between anionic CPF and the negatively charged adsorbent surface as well as competition with OH^- ions led to the decrease in adsorption (Li et al., 2011; Gadipelly et al., 2018). The influence of ionic strength using NaCl on CPF adsorption on the metal complexes is shown Figure 5. A slight decrease in CPF removal from 85 – 76% and 79 – 72% with increase in ionic strength from 0.1 – 0.3 M was obtained for CuHNT and ZnHNT respectively. This is attributed to the competition between Na^+ ions and the cationic CPF species for active sites on the complexes at the solution pH of 6.0 used (Genc et al., 2013). Increasing ionic concentration resulted in decreasing electrostatic interactions between CPF and the adsorbents due to NaCl double layer compression (Mao et al., 2016). Similar result was obtained by some researchers (Zhu et al., 2015; Wang et al., 2017).

Influence of initial pollutant concentration and equilibrium modeling

The initial antibiotic concentration also influences the amount on a given adsorbent. Figure 6 shows the result on the influence of initial CPF concentration on its adsorption onto CuHNT and ZnHNT. A decrease in the percentage abstraction of CPF on both adsorbents was recorded as the initial concentration of the antibiotic increased. In fact as concentration increased from 100 – 500 mg/L a decrease in percentage removal from 91 to 51 and 85 to 45 was obtained for CuHNT and ZnHNT respectively. This result however contradicted that reported by Gadipelly et al (2018) on the sorption of CPF on MOF, where a change in concentration did not significantly affect the adsorption. That may be due to the lower concentration range used in their studies. However, in this case, the decrease in abstraction with concentration may be due to saturation of the adsorbent surface at higher concentration leading to no further removal as concentration increases. The CPF concentration of 100 mg/L was utilized in the adsorption experiments due to optimum removal recorded.

Equilibrium isotherm analysis which helps us understand the mechanism of interaction between the adsorbate and adsorbent was analyzed by the LM, FD and SC models (Akpomie et al., 2015). The equilibrium parameters obtained are presented in Table 1. The regression (R^2) values presented by the LM isotherm were high but that obtained by the FD were higher as R^2> 0.981. The good fit presented by the FD model indicated a heterogeneous surface of CuHNT and ZnHNT involving multilayer CPF adsorption. The suitability of both materials as adsorbents for CPF was evaluated by a LM separation factor R_L. The values of R_L indicates a favorable adsorption (R_L<1) and unfavourable (R_L>1) (Akpomie et al., 2017; El-shafey et al., 2012). The R_L values were in the range of 0.022 – 0.103 for CuHNT and 0.025 – 0.112 for ZnHNT indicating a favorable removal of CPF on the adsorbents. Also, FD n values in the range 2 – 10, 1 – 2, < 1 indicate favorable, moderately difficult and poor abstraction respectively (Sun et al., 2012). The n values for both adsorbents were also in the favourable range which corroborated the deduction of the LM values. The SC model helps to verify the homogenous and heterogeneous surface nature of the adsorbents if a linear plot or deviation from linearity is obtained respectively (Dawodu and Akpomie, 2016). The R^2 values of 0.716 and 0.761 obtained for CuHNT and ZnHNT showed deviation from linearity which supports the deduction of the FD model isotherm of a heterogeneous surface structure of both adsorbents. The maximum monolayer adsorption of ciprofloxacin obtained on both adsorbents was compared with others reported as shown in Table 2. It was observed that the metal complexes of thiourea derivatives of aminophenol showed higher adsorption potential when compared to many adsorbents reported. This establishes the suitability and potential of these metal complexes for adsorption of CPF apart from their medicinal and corrosion inhibition uses.

Effect of agitation time and kinetics on ciprofloxacin removal

The influence of agitation time on the percentage removal of CPF onto CuHNT and ZnHNT is shown in Figure 7. The abstraction process was rapid at the initial stages and increased steadily with agitation time up to 160 min on both sorbent then became constant at equilibrium. The initial abstraction is attributed to higher driving force resulting in faster interaction of ciprofloxacin with the available uncovered active sites on the adsorbents. As time progressed, there was a decrease in driving force and the active sites became covered and saturated therefore CPF molecules slowly diffuses into the pores of the sorbent taking a long time to reach equilibrium (Wu et al., 2015). An agitation time of 240 min was allowed in the adsorption experiment to ensure equilibrium abstraction of CPF was achieved. Kinetic analysis was performed by the PFO, PSO and BH model as shown in Table 3. It was observed that the R^2 presented by the PSO model for both metal complexes were higher than those of the PFO which suggests a chemisorptions process involved in the abstraction of CPF (Li et al., 2015). Furthermore, the good fit (R^2> 0.975) presented by the BH model indicate the involvement of pore diffusion in the abstraction of CPF and this was supported by the high porous structure of CuHNT and ZnHNT obtained from SEM characterization.

Temperature influence, thermodynamics, desorption and reusability

Figure 8 illustrates the effect of solution temperature on the adsorption of CPF on the metal complexes. An increase in percentage abstraction with increase in temperature was obtained for both adsorbent. This suggests an endothermic removal process. The higher abstraction with temperature increase could be attributed to higher diffusion rate of CPF for better interaction with the surface and pores of the adsorbents (Wang et al., 2017). A trend of higher adsorption of CPF on CuHNT than ZnHNT was observed over the experimental factors of pH, concentration,

time and temperature studied. This might be due to the higher surface area and pore volume of the former as a result of better interaction of Zn ions with HNT due to smaller ionic radii (0.72Å) and higher electro-negativity (1.90) compared to 0.74Å and 1.65 for Cu ions respectively. Thermodynamic parameters such as ΔG^0, ΔS^0 and ΔH^0 for the removal process are presented in Table 4. The negative free energy change obtained at the temperature range studied for both CuHNT and ZnHNT indicate a feasible and spontaneous adsorption (Mao et al., 2016). The positive ΔH^0 values supports the endothermic adsorption and positive ΔS^0 is attributed to increased randomness on metal complex-ciprofloxacin interfaces (Dawodu and Akpomie, 2014). The ΔH^0were between the range of physisorption (2.1 – 20.9 kJ/mol) and chemisorptions (80 – 200 kJ/ mol) indicating a physicochemical process. Although desorption studies helps in a clearer classification of the process. If physisorption, significant percentage desorption will be obtained by distilled water while negligible desorption would be achieved in chemisorptions. From desorption studies conducted, only 9.8 and 13.4% desorption of CPF from the surfaces of CuHNT and ZnHNT respectively was achieved using distilled water, while higher desorption of 80.2 and 84.7% using 0.2 M NaOH was achieved for the respective metal complexes. This suggested a chemisorptions mechanism supported by the good fit of the PSO model. Reusability studies showed a decrease in the initial CPF percentage removal from 78.2 to 71.4, 64.3 and 58.1 by CuHNT and from 71.6 to 63.4, 58.7 and 51.2 by ZnHNT for the first second and third cycles respectively. The progressive decrease could be attributed to weight loss of the adsorbents during drying and reuse as well as irreversible binding of some CPF molecules on the active sites of the adsorbents. The high desorption obtained using NaOH as eluent and the reusability indicates the potential of metal complexes of thiourea derivatives as adsorbents for CPX from the environment.

CONCLUSIONS

The copper (II) and Zn (II) complexes of 4-nitro-substituted thiourea derivatives of 2-aminophenol were successfully utilized as adsorbents with high adsorption capacity for ciprofloxacin. Both metal complexes showed high surface area, pore volume and porosity desirable for an efficient adsorbent. Experimental conditions such as pH, ionic strength,initial ciprofloxacin concentration, agitation time and temperature were found to influence the abstraction of ciprofloxacin from aqueous medium. Langmuir and Freundlich constant parameters revealed a favorable adsorption of ciprofloxacin on the adsorbents and kinetics revealed the involvement of pore diffusion in the removal process. Endothermic removal was obtained for both sorbents with a feasible and spontaneous adsorption as revealed by thermodynamic evaluation. Ciprofloxacin molecules were successfully desorbed from the surface of the metal complexes using 0.2 M NaOH and also reused suggesting the potency of the adsorbents for antibiotic removal from aqueous solution.

References

AKPOMIE K. G, EZEOFOR C. C, OLIKAGU C. S, ODEWOLE O. A, & EZEORAH C. J. 2018. Abstraction and regeneration potential of temperature enhanced rice husk montmorillonite combo for oil spill. *Environmental Science and Pollution Research* 25: 34711-34719.

ASHFAQ M, KHAN K.N, RASOOL S, MUSTAFA G, & SAIF-UR-REHMAN M. 2016. Occurrence and ecological risk assessment of fluproquinolone antibiotics in hospital waste of Lahore Pakistan. *Environmental Toxicology and Pharmcology* 42: 16-22.

CARABINEIRO S.A.C, THAVORN-AMORNSRI T, PEREIRA M.F.R, & FIGUEIREDO J.L. 2011. Adsorption of ciprofloxacin on surface-modified carbon materials. *Water Research* 45: 4583-4591.

CHEN D, CHEN J, LUAN X, JI H, & XIA Z. 2011. Characterization of anion-cationic surfactants modified montmorillonite and its application for the removal of methyl orange. *Chemical Engineering Journal* 171: 1150-1158.

CHUKWUEMEKA-OKORIE H.O, EKEMEZIE P.N, AKPOMIE K.G, & OLIKAGU C.S. 2018. Calcined corncob kaolinite combo as new sorbent for sequestration of toxic metal ions from polluted aqua media and desorption. *Frontiers in Chemistry*. 5: 1-13.

DARWEESH T.M, & AHMED M.J. 2017. Adsorption of ciprofloxacin and norfloxacin from aqueous solution onto granular activated carbon in fixed bed column. *Ecotoxicology and Environmental Safety* 128: 139-145.

DAWODU F.A, & AKPOMIE K.G. 2014. Simultaneous adsorption of Ni (II) and Mn (II) ions from aqueous solution unto a Nigerian kaolinite clay. *Journal of Material Research and Technology* 3(2): 129-141.

DAWODU M. O, & AKPOMIE K.G. 2016. Evaluating the potential of a Nigerian soil as an adsorbent for tartrazine dye: isotherm kinetic and thermodynamic studies. *Alexandria Engineering Journal* 55: 3211-3218.

DE OLIVEIRA C.G.M, FARIA V.W, ANDRADE G.F, D'ELIA E, CABRAL M.F, COTRIM B.A, RESENDE G.O, & DE SOUZA F. C. 2015. Synthesis of thiourea derivatives and its

evaluation as corrosion inhibitor for carbon steel. *Phosphorous Sulfur Silicon and Related Elements* doi.org/10.1080/10426507.2015.1035719.

EL-SHAFEY E.I, AL-LAWATI H, & AL-SUMRI A.S. 2012. Ciprofloxacin adsorption from aqueous solution onto chemically prepared carbon from date palm leaflets. *Journal of Environmental Sciences* 24(9): 1579-1586.

ELWAKEEL K. Z, & AL-BOGAMI A. S. 2018. Influence of Mo (VI) immobilization and temperature on As (V) sorption onto magnetic seperable poly p-phenylenediamine-thiourea formaldehyde polymer. *Journal of Hazardous Materials* 342: 335-346.

ELWAKEEL K. Z, EL-BINDARY A. A, ISMAIL A, & MORSHIDY A. M. 2017. Magnetic chitosan grafted with polymerized thiourea for remazol brilliant blue R recovery: effects of uptake conditions. *Journal of Dispersion Science and Technology* 38: 943-952.

EZE, S. I., AKPOMIE K. G, EZEOFOR C. C, OSUNKUNLE A. A, MADUEKWE O. B & OKENYEKA O. U. 2019. Isotherm and kinetic evaluation of *Dialium guineense* seed husk and its modified derivatives as efficient sorbent for crude oil polluted water treatment. *Water Conservation Science and Engineering* doi.org/10.1007/s41101-019-00065-6.

FAYOMI O. M, SHA'ATO R, WUANA R. A, IGOLI J. O, MOODLEY V, & VAN ZYL W. E. 2018a. Synthesis, characterization and antibacterial studies of some metal complexes of *N*-di (pyridin-2-yl) thiourea derivatives. *International Research Journal of Pure and Applied Chemistry* 16 (32): 1-31.

FAYOMI O. M, SHA'ATO R,WUANA A, IGOLI J. O, MOODLEY V, & VAN ZYL W E. 2018B. Spectroscopic and antibacterial studies of some nitro-substituted *N*-

(benzoylcarbamothioyl) amino acids: the crystal structure of *N*-(3-nitro-benzoylcarbamothioyl)-glycine. *Journal of Chemical Society of Nigeria* 43 (2): 119-132.

GADIPELLY C.R, MARATHE K.V, & RATHOD V.K. 2018. Effective adsorption of ciprofloxacin by hydrochloride from aqueous solution using metal organic framework. *Separation Science and Technolology* doi.org/10.1080/01496395.2018.1474225.

GENC N, DOGAN E. C, & YURTSEVER M. 2013. Bentonite for ciprofloxacin removal from aqueous solution. *Water Science and Technology* 68(4): 848-855.

GEZER N, GULFEN M, & AYDIN A.O. 2011. Adsorption of selenite and selenate ions onto thiourea-formaldehyde resin. *Journal of Applied Polymer Science* 122: 1134-1141.

HASAN Z, & JHUNG S.H. 2015. Removal of hazardous organics from water using metal organic frameworks (MOfs): plausible mechanisms for selective adsorption. *Journal of Hazardous Material* 283: 329-338.

HUANG L, WANG M, SHI C, HUANG J, & ZHANG B. 2014. Adsorption of tetracycline and ciprofloxacin on activated carbon prepared from lignin with H3PO4 activation. *Desalination and Water Treatment* 52: 2678-2697.

KHAN A, WANG J, LI J, WANG X, CHEN Z, ALSAEDI A, HAYAT T, CHEN Y, WANG X. 2017. The role of grapheme oxide and grapheme oxide-based nanomaterials in the removal of pharmaceuticals from aqueous media: a review. Environmental Science and Pollution Research 24: 7938-7958.

LI H, ZHANG D, HAN X, & XING B. 2014. Adsorption of antibiotic ciprofloxacin on carbon nanotubes: pH dependence and thermodynamics. Chemosphere 95: 150-155.

LI X, WANG W, DOU J, GAO J, CHEN S, QUAN X, & ZHAO H. 2015. Dynamic adsorption of ciprofloxacin on carbon nanofibers: quantitative measurement by insitu fluorescence. *Journal of Water Process Engineering* doi.org/10.1016/j.jwpe.2014.12.006.

LI Z, HONG H, LIAO L, ACKLEY C.J, SCHULZ L.A, MAC-DONALD R.A, MIHELICH A.L, & EMARD S.M. 2011. A mechanistic study of ciprofloxacin removal by kaolinite. *Colloid and Surfaces B-Biointerfaces* 88: 339-344.

LIANG Z, ZHAO Z, SUN T, SHI W, & CUI F. 2016. Adsorption of quinolone antibiotics in spherical mesoporous silica effects of the retained template and its alkyl chain length. *Journal of Hazardous Material* 305: 8-14.

MAO H, WANG S, LIN J.Y, WANG Z, & REN J. 2016. Modification of a magnetic carbon composite for ciprofloxacin adsorption. *Journal of Environmental Sciences* 49: 179-188.

MUSLU N, & GULFEN M. 2011. Selective separation and concentration of Pd (II) from Fe (III), Co (II), Ni (II) and Cu (II) ions using thiourea-formaldehyde resin. *Journal of Applied Polymer Science* 120: 3316-3324.

OMOREGIE H. O, FAYOMI O. M, ADELEKE O. E, & WOODS J. A. O. 2013. Synthesis, spectroscopic properties and antimicrobial studies of copper (II) complexes with N-donor heterocyclic ligands. *Science Focus*18 (1): 36-43.

PARMAR S, KUMAR Y, & MITTAL A. 2010. Synthesis, spectroscopic and pharmacological studies of bivalent copper, zinc and mercury complexes of thiourea. *South African Journal of Chemistry* 63:1-7.

POURETEDAL H.R, & SADEGH N. 2014. Effective removal of amoxicillin, cephalexin, tetracycline and penicillin G from aqueous solution using activated carbon nanoparticles prepared from vine wood. *Journal of water Process Engineering* 1: 64-73.

SELVAKUMARAN N, PRATHEEPKUMAR A, NG S.W, TIEKINK E.R.T, & KARVEMBU R. 2013. Synthesis, structural characterization and cytotoxicity of nickel (II) complexes containing 3,3-dialkyl/aryl-1-benzoylthiourea ligands. *Inorganic Chimica Acta* 404: 82-87.

SHI S, FAN Y, & HUANG Y. 2013. Facile low temperature hydrothermal synthesis of magnetic mesoporous carbon nano composite for adsorption removal of ciprofloxacin antibiotics. *Industrial and Engineering Chemistry Research* 52(7): 2604-2612.

STURINI M, SPELTINI A, MARASCHI F, PRETALI L, PROFUMO A, FASANI E, ALBINI A, MIGLIAVACCA R, & NUCLEO E. 2012. Photodegradation of fluoroquinolones in surface water and antimicrobial activity of the photo products. *Water Research* 46(17): 5575-5582.

STURINI M, SPELTINI A, MARASCHI F, PROFUMO A, & TARANTINO S. 2016. Removal of fluoroquinolone contaminants from environmental waters on sepiolite and its photo induced regeneration. *Chemosphere* 150: 686-693.

SUN Y, YUE Q, GAO B, HUANG L, XU X, & LI Q. 2012. Comparative study on characterization and adsorption properties of activated carbons with H_3PO_4 and $H_4P_2O_7$ activation employing cyperus alternifolius as precursor. *Chemical Engineering Journal* 181: 790-797.

WANG C.J, LI Z.H, JIANG W.T, JEAN J.S, & CHUAN C.C. 2010. Cation exchange interaction between antibiotic ciprofloxacin and monymorillonite. *Journal of Hazardous Material* 183(1-3): 309-314.

WANG M, LI G, HUANG L, XUE J, LIU Q, BAO N & HUANG J. 2017. Study of ciprofloxacin adsorption and regeneration of activated carbon prepared from Enteromorpha prolifera impregnated with H_3PO_4 and sodium benzenesulfonate. *Ecotoxicology and Environmental Safety* 139: 36-42.

WU Q, LI Z, HONG H, YIN K, & TIE L. 2010. Adsorption and intercalation of ciprofloxacin on montmorillonite. *Applied Clay Science* 50(2): 204-211.

WU S, LI Y, ZHAO X, DU Q, WANG Z, XIA Y, & XIA L. 2015. Biosorption behavior of ciprofloxacin onto Enteromorpha prolifera: isotherm and linetic studies. *International Journal of Phytoremediation* 17: 957-961.

WU Y, PANG H, LIU Y, WANG X, YU S, FU D, CHEN J, & WANG X. 2019. Environmental remediation of heavy metal ions by novel nanomaterials: a review. *Environmental Pollution* 246: 608-620.

YU F, LI Y, HAN S, & MA J. 2016a. Adsorptive removal of antibiotics from aqueous solution using carbon materials. *Chemsosphere* 153: 365-385.

YU F, SUN S, HAN S, ZHENG J, & MA J. 2016b. Adsorption removal of ciprofloxacin by multi-walled carbon nanotubes with different oxygen contents from aqueous solution. *Chemical Engineering Journal* 285: 588-595.

ZHANG C.L, QIAO G.L, ZHAO F, & WANG Y. 2011. Thermodynamic and kinetic parameters of ciprofloxacin adsorption onto modified coal fly ash from aqueous solution. *Journal of Molecular Liquids* 163 (1): 53-56.

ZHU X, TSANG D. C. W, CHEN F, LI S, & YANG X. 2015. Ciprofloxacin adsorption on grapheme and granular activated carbon: kinetics, isotherms and effects of solution chemistry. *Environmental Technology* doi.org/10.1080/09593330.2015.1054316.

SCHEMES

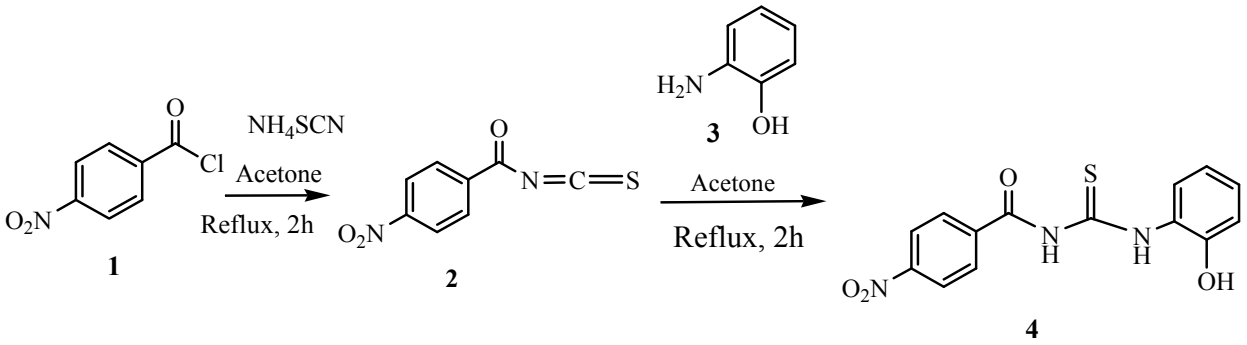

Scheme 1: Synthesis of *N-(2-hydroxylphenyl)-N'-(4-nitro benzoyl) thiourea*(HNT)**(4)**

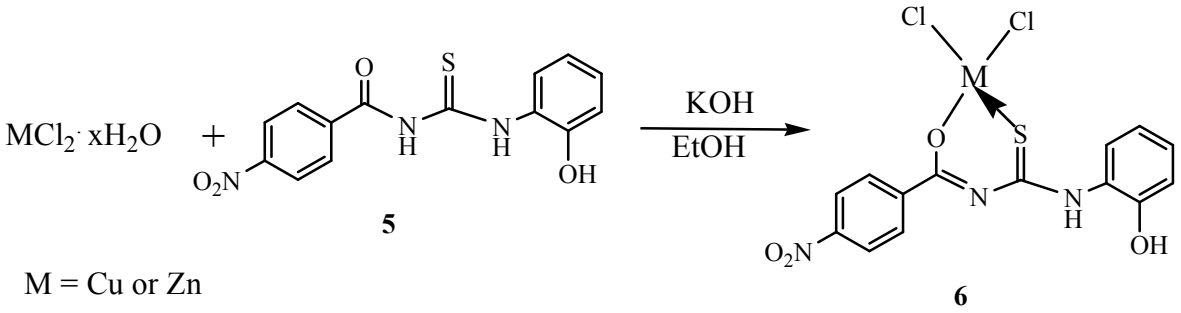

Scheme 2: Synthetic pathway Cu (II) and Zn (II) metallic complexes of *thiourea derivatives of aminophenols*

TABLES

Table 1: Equilbrium isotherm constants for abstraction of ciprofloxacin on metal complexes.

Isotherm Model	CuHNT	ZnHNT
Langmuir		
q_L (mg/g)	238.2	231.3
K_L (L/mg)	0.087	0.079
R^2	0.923	0.918
Freundlich		
K_F (mg/g)	11.7	9.8
n	2.26	2.44
R^2	0.982	0.991
Scatchard		
qs (mg/g)	292.4	281.6
b (L/mg)	0.085	0.077
R^2	0.716	0.761

Table 2: Maximum monolayer uptake capacities of different adsorbents for ciprofloxacin

Adsorbent	q_{max} (mg/g)	Reference
Montmorillonite	395	Wang et al., 2011
Montmorillonite	330	Wang et al., 2010
Modified coal fly ash	1.55	Zhang et al., 2011
Oxidized xerogel	60	Carabinero et al., 2011
Kaolinite	6.3	Li et al., 2011
Illite	33	Wang et al., 2011
Rectorite	135	Wang et al., 2011
Wet prepared carbon	133.3	El-shafey et al., 2012
Dry prepared carbon	125.0	El-Shafey et al., 2012
Geothite	49.8	El-Shafey et al., 2012
Aluminous oxide	13.6	El-Shafey et al., 2012
Magnetic mesoporous	98.3	Shi et al., 2013
Fe_2O_4/C adsorbent	90.1	Mao et al., 2016
Activated carbon (AC)	244	Wang et al., 2017
Modified AC (AC-SBS)	286	Wang et al., 2017
Regenerated AC	233	Wang et al., 2017
Regenerated AC-SBS	256	Wang et al., 2017
Multiwalled carbon nanotubes	150 – 206	Yu et al., 2016b
CuHNT	238.2	This work
ZnHNT	231.3	This work

Table 3: Kinetic constants for uptake of ciprofloxacin on the metal complexes

Kinetic Model	CuHNT	ZnHNT
Pseudo-first-order		
qe (mg/g)	134.3	117.8
K_i (min^{-1})	0.016	0.023
R^2	0.971	0.982
Pseudo-second-order		
qe (mg/g)	178.8	162.3
K_2 (mg/g min)	2.6×10^{-5}	4.3×10^{-5}
R^2	0.996	0.992
Bangham		
a_B	0.631	0.644
K_o	4.42	6.71
R^2	0.981	0.976

Table 4: Thermodynamic constants for ciprofloxacin uptake by the metal complexes

Thermodynamic parameters	CuHNT	ZnHNT
300K (ΔG°) (KJ/mol)	−3.12	−3.01
313K (ΔG°) (KJ/mol)	−3.31	−3.23
323K (ΔG°) (KJ/mol)	−3.48	−3.34
ΔH° (KJ/mol)	38.61	35.12
ΔS° (J/mol K)	70.4	68.6

FIGURES

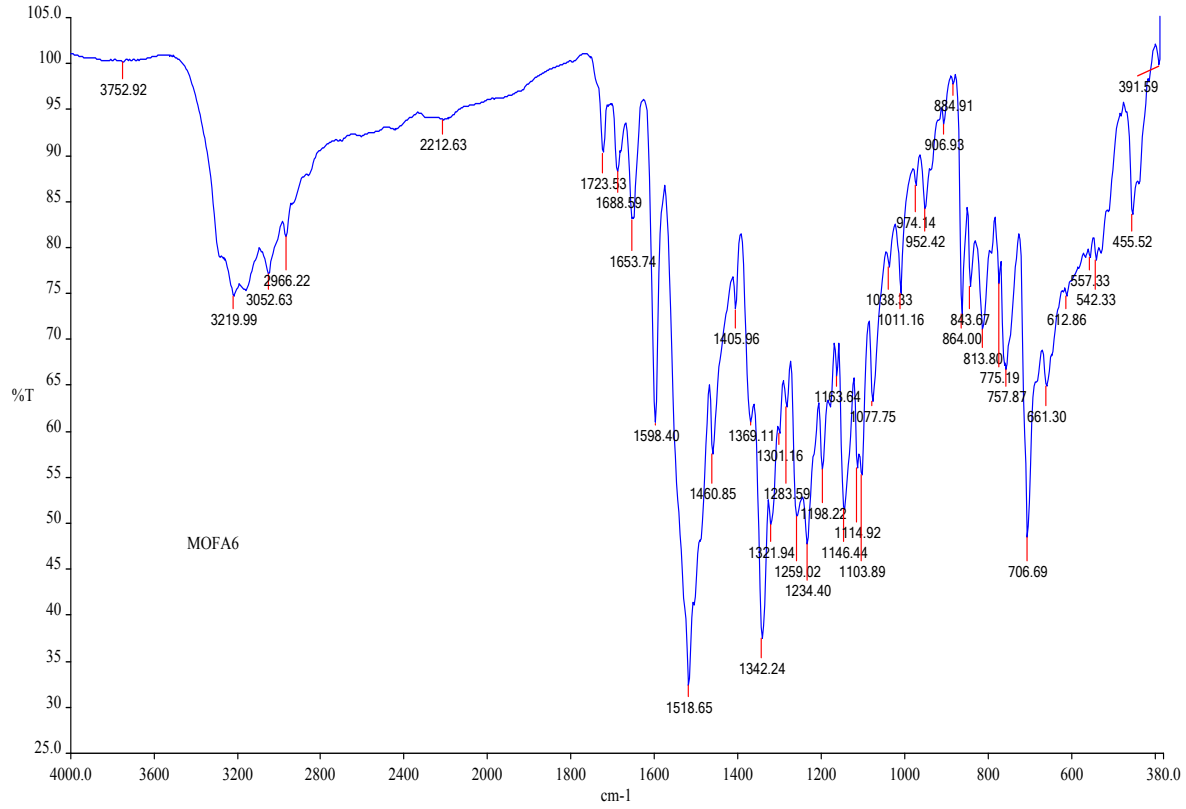

Figure 1: FTIR spectra of HNT

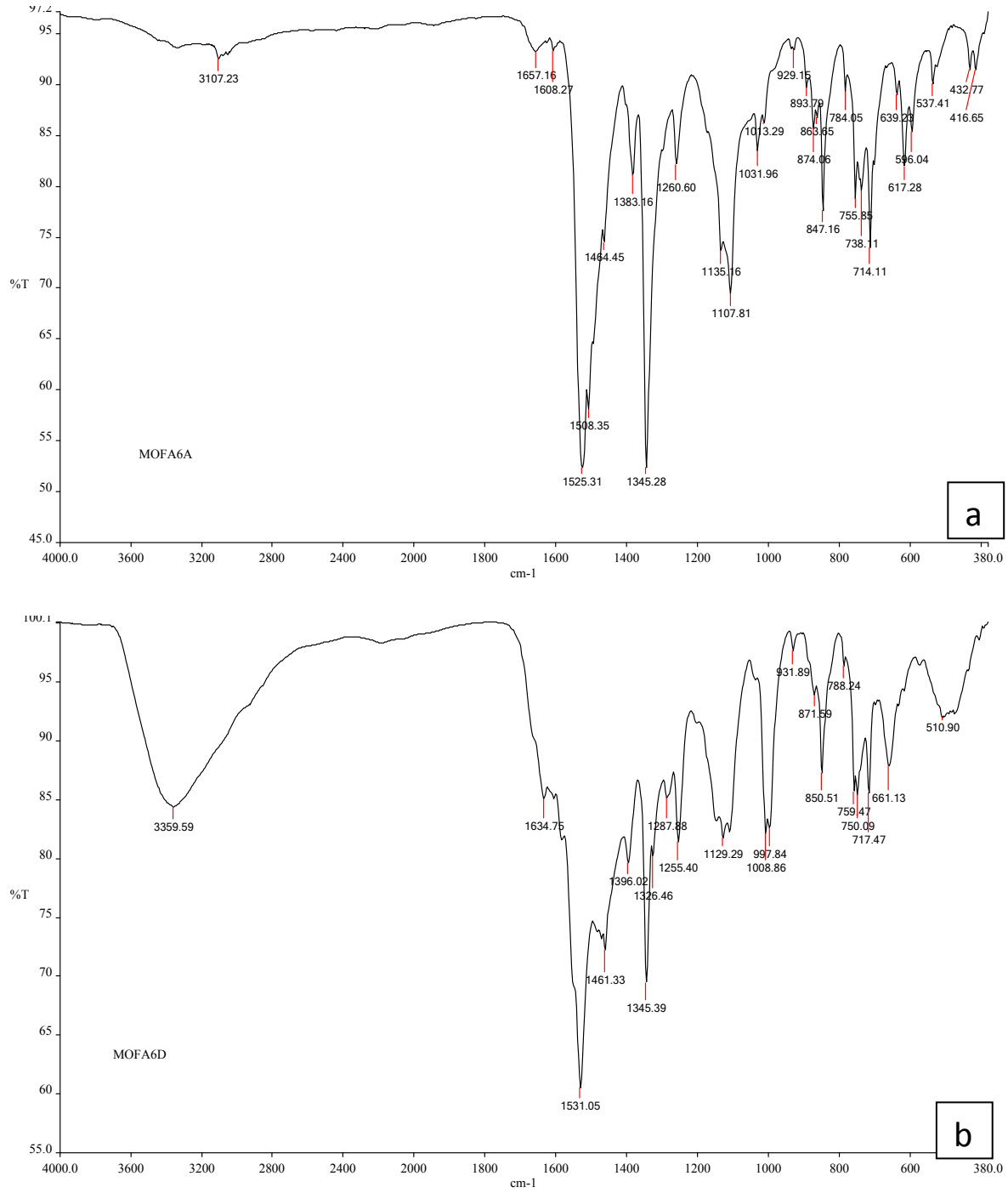

Figure 2: FTIR spectra of (a) CuHNT and (b) ZnHNT

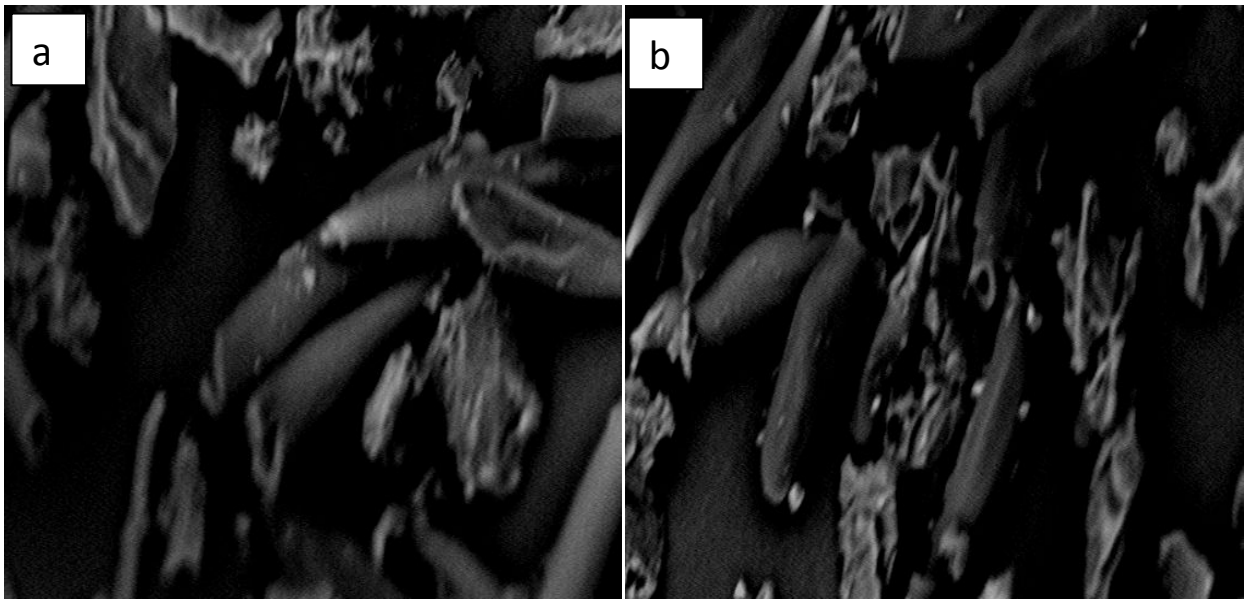

Figure 3: SEM images of (a) CuHNT and (b) ZnHNT

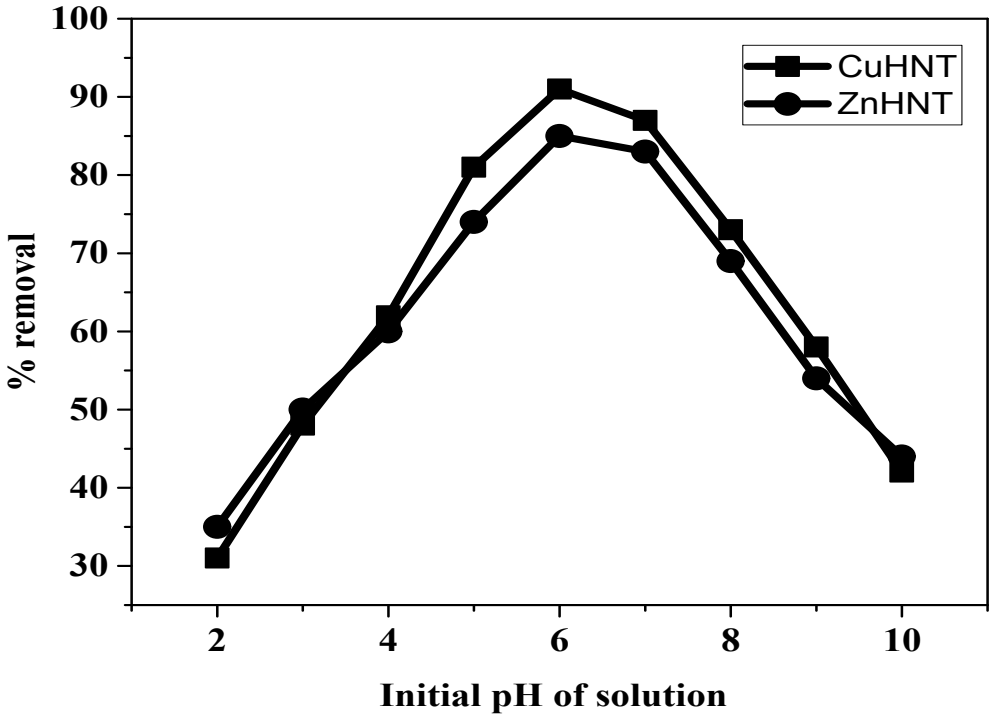

Figure 4: Influence of initial pH of solution on ciprofloxacin adsorption by the metal complexes

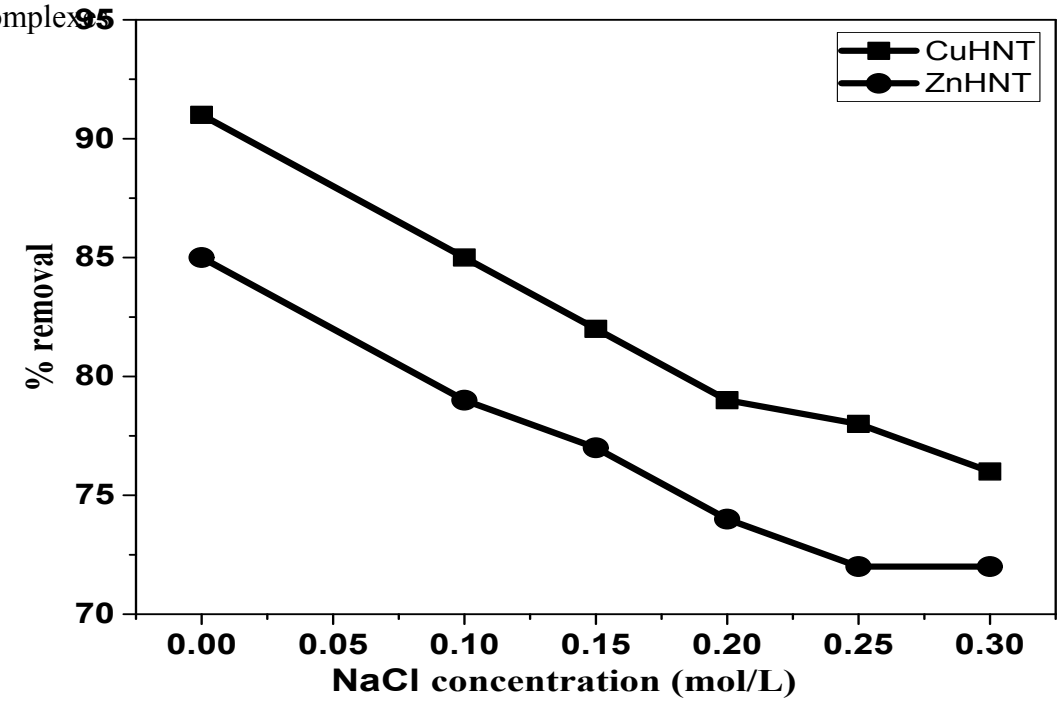

Figure 5: Influence of ionic strength on ciprofloxacin adsorption by the metal complexes

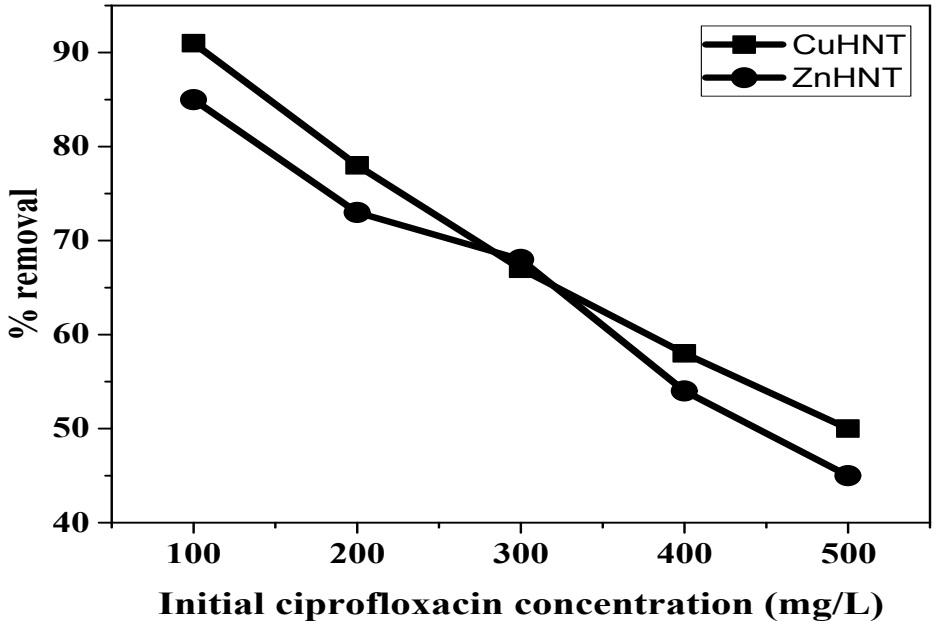

Figure 6: Influence of initial concentration on ciprofloxacin adsorption by the metal complexes

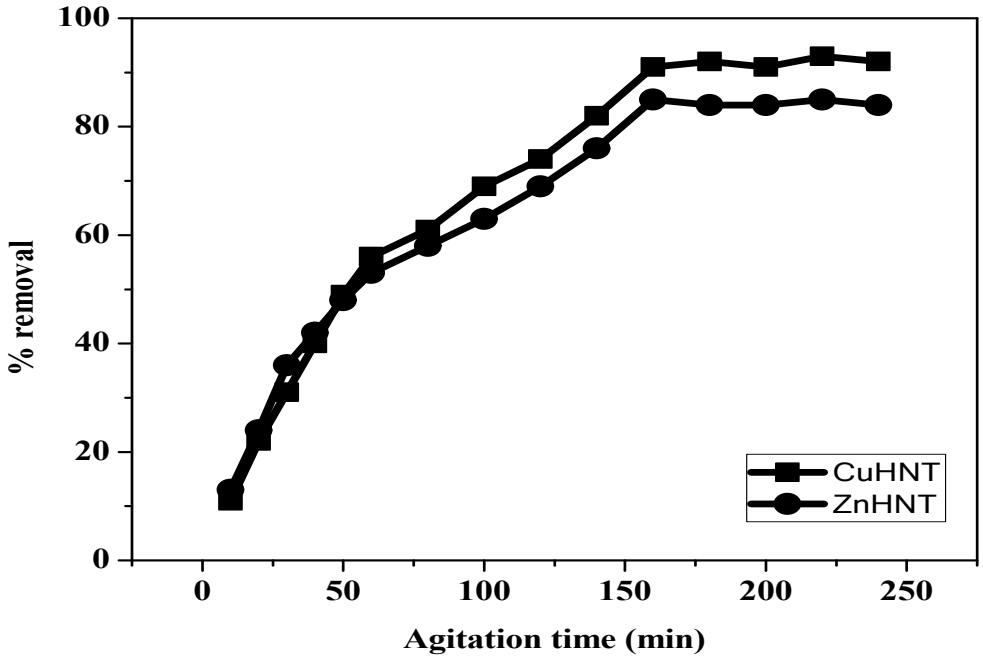

Figure 7: Influence of agitation time on ciprofloxacin adsorption by the metal complexes

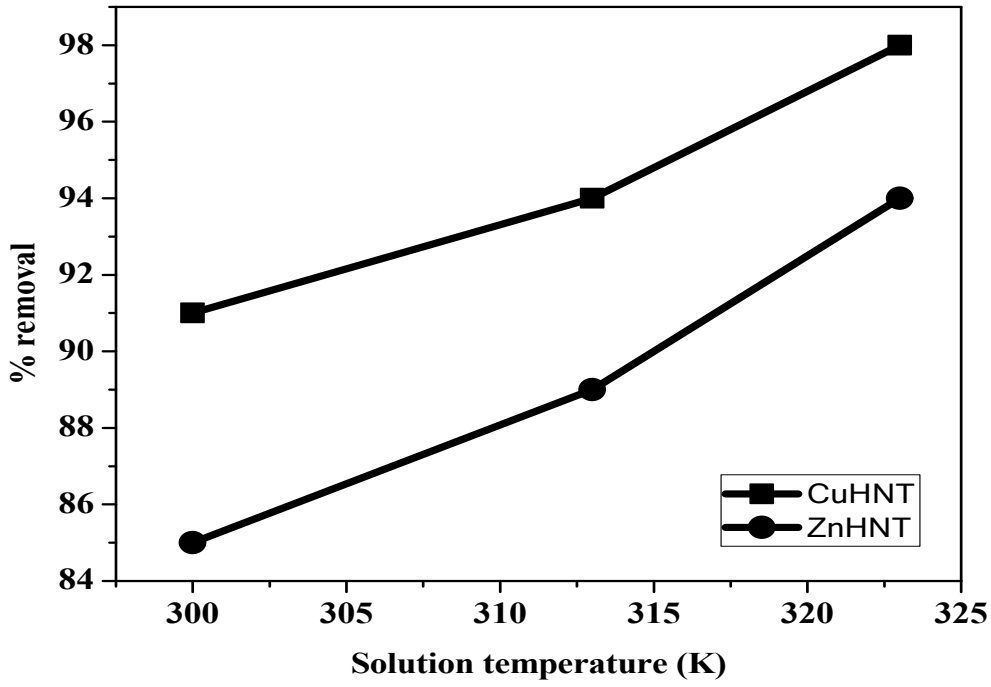

Figure 8: Influence of solution temperature on ciprofloxacin adsorption by the metal complexes